Journal of the European Ceramic Society 23 (2003) 865–871

www.elsevier.com/locate/jeurceramsoc

Effects of cobalt-ion doping on the electrochemical properties of spinel lithium manganese oxide prepared via a reverse-micelle route

Chung-Hsin Lu*, Hsien-Cheng Wang

Department of Chemical Engineering, National Taiwan University, Taipei 106, Taiwan, ROC

Received 28 November 2001; received in revised form 7 June 2002; accepted 16 June 2002

Abstract

Monophasic, ultrafine cobalt ion-doped lithium manganate powders have been prepared via a reverse-micelle process. $LiMn_{1.8}Co_{0.2}O_4$ powders were obtained after heating at 500 °C for 2 h. Both the required reaction temperature and duration for synthesizing this compound were greatly reduced, compared to those in the conventional technique involving solid-state reaction. Increasing the water to oil (W/O) volume ratio resulted in an increase in the particle size of $LiMn_{1.8}Co_{0.2}O_4$ as well as the formation of impure Li_2MnO_3 phase. Nanosized, monophasic powders were obtained when the W/O volume ratio was 1/5. Raising the heating temperature led to an increase in the crystallite size as well as the particle size of $LiMn_{1.8}Co_{0.2}O_4$. Based on the analytic results of electrochemical properties, the derived cobalt ion-doped spinel phase was confirmed to exhibit moderate discharge capacity and improved cycleability at ambient as well as elevated temperatures.

Keywords: Batteries; Electrochemical properties; $Li(Mn,Co)_2O_4$; Lithium batteries; Spinels

1. Introduction

Lithium-ion secondary batteries have drawn great attention in the field of portable devices due to their high working voltage, low self-discharge rate, elevated energy density, and long shelf life.[1–4] In lithium ion batteries, several lithiated powders, such as layer-structured $LiCoO_2$, $LiNiO_2$, and spinel-structured $LiMn_2O_4$, are usually adopted as the cathode materials. Among these cathode materials, $LiMn_2O_4$ is the most promising candidate owing to the inexpensive material cost of manganese compound, acceptable environmental characteristics, and better safety.[5,6] However, $LiMn_2O_4$ suffers a severe capacity fading problem after long-term cycling which limits its application to Li-ion batteries. The capacity fading may be attributed to several mechanisms such as tetragonal distortion caused by Jahn-Teller effect,[2,5] dissolution of active materials in the positive electrodes,[6,7] electrochemical instability of the electrolyte charging at high voltages,[8,9] and the passive film formation on the electrodes.

For improving the cycleability of $LiMn_2O_4$, doping of other cations into $LiMn_2O_4$ has been intensively investigated.[10–12] The spinel compound can be stabilized by doping M (III) cations into the host structure during the processes of intercalation and deintercalation of lithium ions. In the previous studies, cobalt ions have been found to be an effective dopant for improving the electrochemical performance of $LiMn_2O_4$.[12–15] Cobalt ion-doped lithium manganate powders have been prepared using the solid-state reaction, sol-gel methods and precipitation techniques;[16–18] nevertheless, these methods resulted in powders with large particle size and less controlled morphology. In order to obtain ultrafine and uniform cathode powders, a reverse-micelle process has been developed in this study. This process has been found to be a promising method for synthesizing nanosized ceramic powders.[19–23] Reducing the particle size and increasing the specific surface area of cathode materials will shorten the diffusing length of lithium ions during the intercalation/de-intercalation process, thereby improving the electrochemical performance. In this study, the aqueous phase containing manganese,

---

* Corresponding author. Tel.: +886-2-363-5230; fax: +886-2-362-3040.

E-mail address: chlu@ccms.ntu.edu.tw (C.-H. Lu).

0955-2219/03/$ - see front matter © 2002 Elsevier Science Ltd. All rights reserved.
PII: S0955-2219(02)00209-1

cobalt, and lithium cations with an appropriate ratio was dispersed into the oil phase. By introducing a specific surfactant and emulsifying treatment into this system, the aqueous phase was thoroughly dispersed to form discrete micelles in the oil phase. Since each micelle acts as an independent reactor, the morphology and size of the formed powders can be manipulated by the size of micelles. Fine cobalt ion-doped $LiMn_2O_4$ powders were prepared via the reverse-micelle process, and the effects of the volume ratio of water to oil on the electrochemical properties were examined. It was found that the obtained powders exhibited not only good discharge capacities, but also enhanced cycling performance at ambient temperature as well as elevated temperatures.

2. Experimental

Three types of emulsion systems were prepared. The water to oil (W/O) volume ratios were adjusted to be 1/5 (system I), 1/1 (system II), and 2/1 (system III). Kerosene was chosen to be the oil phase, and sorbitan monooleate (Span 80, Aldrich Co. USA) was used as the surfactant to increase the stability of the emulsified system. The amount of Span 80 was fixed to be 5 vol.% of the total volume of oil and aqueous phases. Aqueous phase was prepared by dissolving appropriate amounts of lithium acetate, manganese acetate and cobalt acetate in deionized water. In order to achieve good cycling performance and high discharge capacity, the ratio of Li:Mn:Co was set to be 1:1.8:0.2. The concentration of the aqueous solution was maintained at 1 M with respect to all cations. After mixing the prepared aqueous phase with the oil phase, the mixed solution was agitated for 1 h using a homogenizer at a spinning rate of 6000 rpm to obtain the well-emulsified solution. Then the solution was dropped into hot kerosene (170–180 °C) slowly and later dried at 300 °C for 1 h to obtain the precursor powders.

For elucidating the phase development, the precursor powders were heated at elevated temperatures from 500 to 800 °C for 2 h, and the crystal structures of the heated specimens were examined using powder X-ray diffraction (XRD) analysis that employed a Mac X-ray powder diffractometer. The crystallite size of the calcined powder was calculated from the broadening at half maximum of the (111) diffraction peak of $LiMn_{1.8}Co_{0.2}O_4$ based on the Scherrer equation.[24] The lattice parameters were calculated by the least-square method. The particle size and microstructural morphology of the precursor and calcined powders were examined using transmission electron microscopy (TEM) (Hitachi H7100).

The electrochemical characteristics of the obtained powders were investigated by charging and discharging the test cells. The composite cathode contained a mixture of $LiMn_{1.8}Co_{0.2}O_4$ powders, carbon black, and polyvinylidene difluoride (PVDF) binder. The electrolyte consists of 1 M solution of $LiPF_6$ dissolved in (1:1) mixture of ethylene carbonate (EC) and dimethyl carbonate (DMC). Test cells were assembled in a glove box filled with extremely pure argon. All the electrochemical cycling studies were galvanostatically undertaken at a constant current density of 0.23 mA/cm^2 within the range of 3.0–4.2 V.

3. Results and discussion

3.1. Formation of the reverse-micelle derived $LiMn_{1.8}Co_{0.2}O_4$ powders

The XRD patterns of the calcined powders prepared by the reverse-micelle process in system I are illustrated in Fig. 1. All the calcined powders were confirmed to exhibit a spinel structure. Monophasic $LiMn_{1.8}Co_{0.2}O_4$ was formed at as low as 500 °C. When the calcination temperature reached 800 °C, the well-crystallized spinel compound was obtained. Heating at higher temperatures resulted in an increase in the crystallinity of $LiMn_{1.8}Co_{0.2}O_4$. In the conventional solid-state process, the pure compound of $LiMn_{1.8}Co_{0.2}O_4$ was synthesized after heating at 800 °C for 10 h.[16] On the other hand, the required heating time for the reverse-micelle derived precursors was significantly shortened to merely 2 h. The above results confirm that the reverse-micelle process

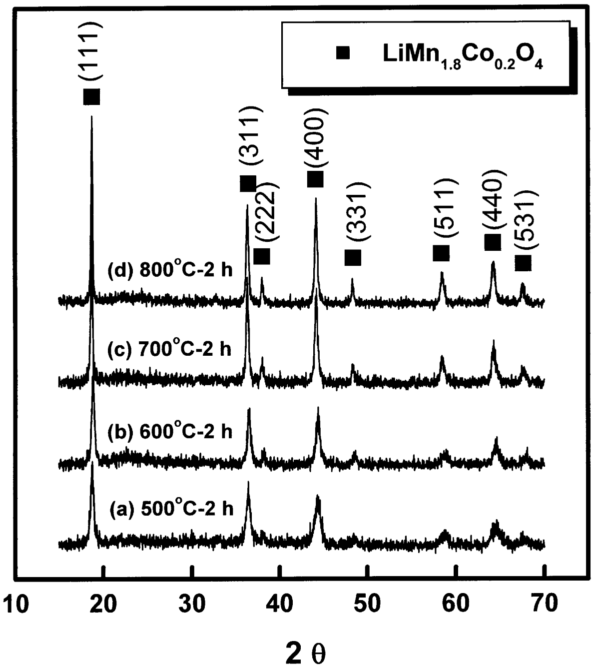

Fig. 1. XRD patterns of the reverse-micelle derived precursors prepared at a W/O volume ratio of 1/5 after calcination at (a) 500 °C, (b) 600 °C, (c) 700 °C, and (d) 800 °C for 2 h.

can greatly curtail the calcination time for synthesizing $LiMn_{1.8}Co_{0.2}O_4$ powders.

Fig. 2 illustrates the respective XRD patterns of the calcined specimens in system II and system III at 800 °C. In both systems, a small amount of the impure Li_2MnO_3 phase was detected other than the spinel compound. The relative percentages of the spinel phase in the three systems are illustrated in Fig. 3. The amount of the spinel $LiMn_{1.8}Co_{0.2}O_4$ phase was estimated based on the relative intensity of the major diffraction peaks of the spinel and the Li_2MnO_3 phases via the following equation:

$$X_{LMO} = \frac{I_{LMO}(111)}{I_{LMO}(111) + I_{MO}\left(\bar{1}33\right)} \quad (1)$$

I_{LMO} refers to the intensity of the spinel (111) peak and I_{MO} represents the intensity of the Li_2MnO_3 $(\bar{1}33)$ peak. It was found that the percentages of spinel phase decreased with increasing the water to oil (W/O) volume ratio. Monophasic $LiMn_{1.8}Co_{0.2}O_4$ was obtained only at a W/O volume ratio of 1/5 at all of the examined temperature range. The W/O volume ratio appeared to be a predominant factor for synthesizing pure $LiMn_{1.8}Co_{0.2}O_4$.

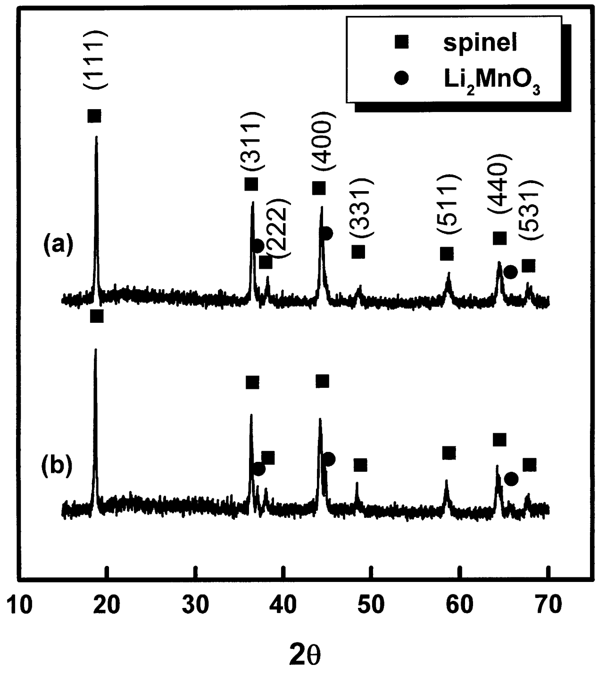

Fig. 2. XRD patterns of the 800 °C-calcined powders obtained at a W/O volume ratio of (a) 1/1 and (b) 2/1, respectively.

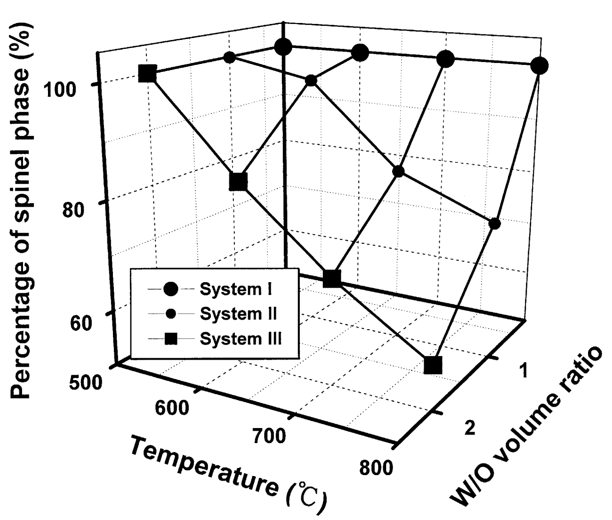

Fig. 3. Three-dimensional presentation of the percentage of the spinel $LiMn_{1.8}Co_{0.2}O_4$ phase.

For investigating the effects of W/O volume ratio on the formation of $LiMn_{1.8}Co_{0.2}O_4$, the stability of the prepared emulsion was examined by measuring the separation time of the aqueous and the oil phases. When the W/O volume ratio was 2/1, the separation time was merely 20 s. As the W/O volume ratio decreased to 1/1, the separation time increased to 1 min. The separation time was greatly prolonged to 20 min when the W/O volume ratio equaled 1/5. The above results revealed that the stability of the emulsion system was significantly enhanced by decreasing the W/O volume ratio. At a high W/O volume ratio, the emulsion system became unstable, so that the aqueous phase was not able to evenly disperse in the oil phase, thereby resulting in the inhomogeneity of the precursors and the formation of the impure phase.

3.2. Microstructure of the reverse-micelle derived $LiMn_{1.8}Co_{0.2}O_4$ powders

The average crystallite size of $LiMn_{1.8}Co_{0.2}O_4$ versus the calcination temperature from 500 to 800 °C is shown in Fig. 4. It was found that the crystallite sizes of the 500 °C-calcined specimens of system I, II, and III were 25, 31, and 34 nm, respectively. Raising temperature monotonously increased the crystallite size for all systems. When the calcination temperature was raised to 800 °C, the sizes of the specimens obtained from system I, II, and III were 38, 74, and 87 nm, respectively. It was found that large W/O volume ratio resulted in an increase in the crystallite size. The microstructures of the calcined $LiMn_{1.8}Co_{0.2}O_4$ powders in system I are shown in Fig. 5. The average particle size of the 600 °C-calcined powders was 32 nm [Fig. 5 (a)], whereas that of the 800 °C-calcined powders increased to 98 nm [Fig. 5 (c)]. These results demonstrate that nanosized $LiMn_{1.8}Co_{0.2}O_4$ powders were prepared via the reverse-micelle process.

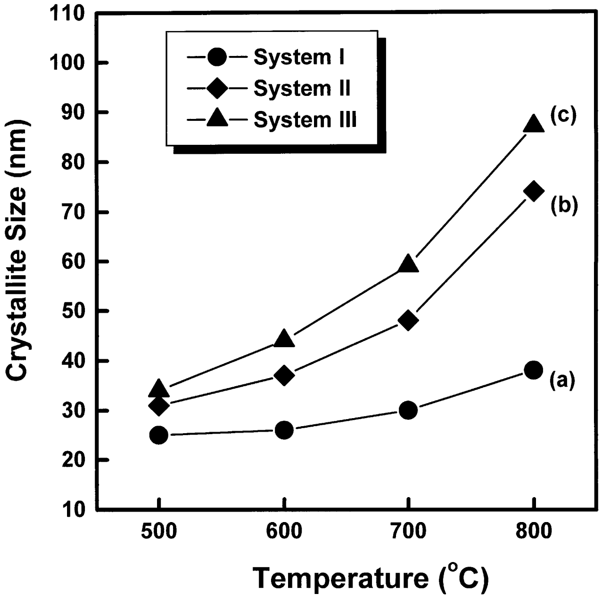

Fig. 4. Crystallite size of the calcined powders obtained at a W/O volume ratio of (a) 1/5, (b) 1/1, and (c) 2/1.

On the other hand, the particle size of the heated powders increased with a rise in the W/O volume ratio. As shown in Fig. 6(a), the average size of the 800 °C-calcined sample in system II was 117 nm. Once the W/O volume ratio further increased to 2/1 as in system III, the average particle size greatly increased to 138 nm [Fig. 6(b)]. For the sol-gel derived $LiMn_{1.8}Co_{0.2}O_4$, the average particle size of 800 °C-calcined specimen was around 1 μm.[25] Therefore, the particle size of $LiMn_{1.8}Co_{0.2}O_4$ powders prepared via this method is much smaller than that of powders obtained by the sol-gel process. In the reverse-micelle process, numerous tiny micelles were generated with intense agitation in the emulsifying process. After calcining the emulsified precursors, the tiny micelles resulted in the formation of fine powders. When the W/O volume ratio increased, the emulsion system became unstable, and part of the formed micelles tended to coagulate to form large droplets. Therefore, a high W/O volume ratio resulted in the formation of large $LiMn_{1.8}Co_{0.2}O_4$ particles.

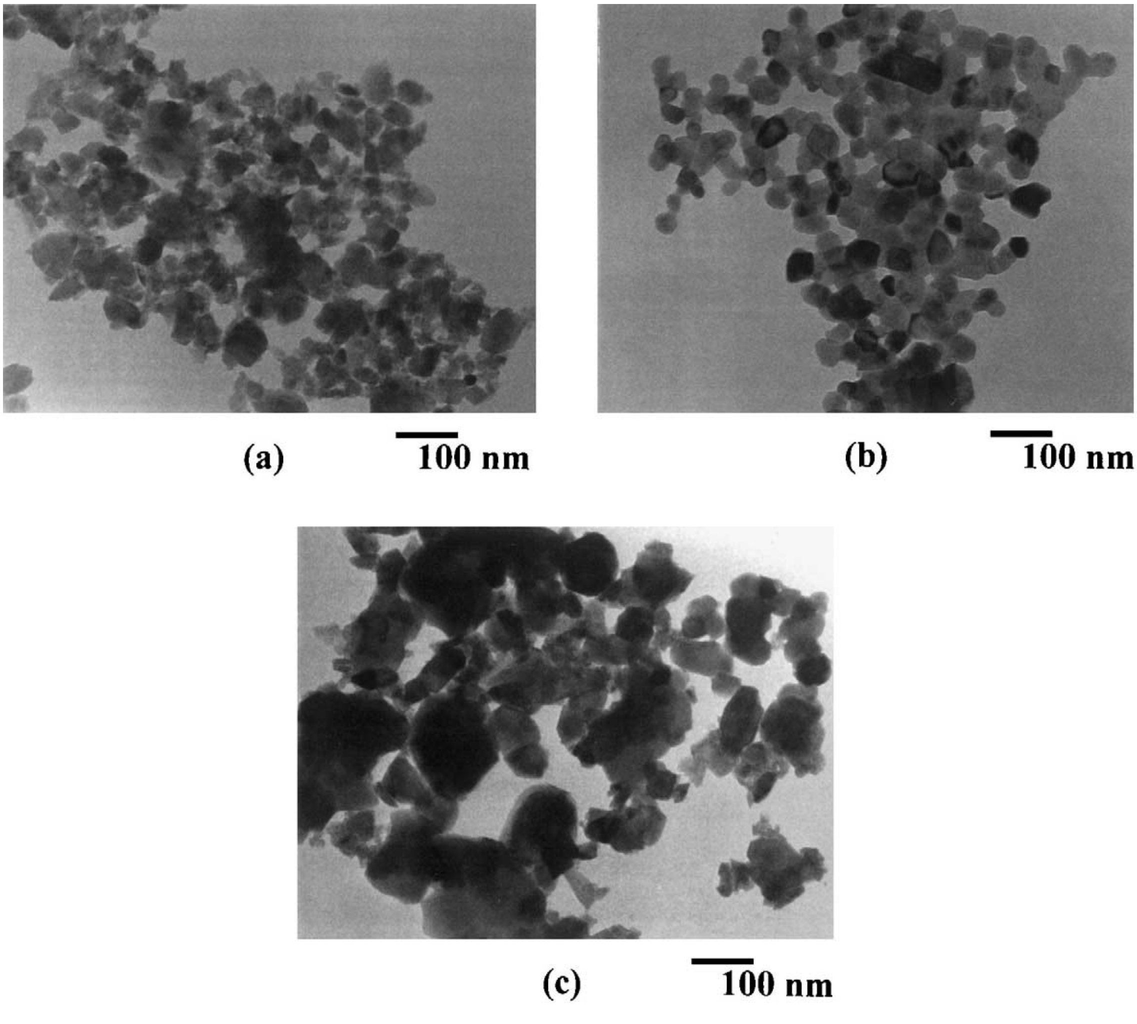

Fig. 5. TEM photos of the calcined $LiMn_{1.8}Co_{0.2}O_4$ powders calcined at (a) 600 °C, (b) 700 °C, and (c) 800 °C in system I.

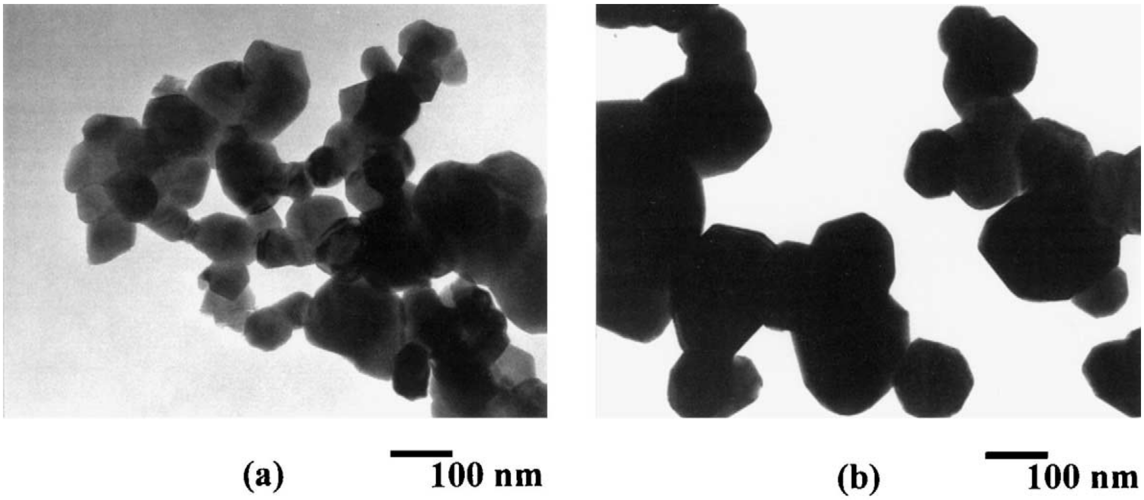

Fig. 6. TEM photos of the 800 °C-calcined $LiMn_{1.8}Co_{0.2}O_4$ powders prepared at a W/O volume of (a) 1/1 and (b) 2/1.

3.3. *Electrochemical properties of the reverse-micelle derived $LiMn_{1.8}Co_{0.2}O_4$ powders*

The room-temperature charge and discharge curves of 800 °C-calcined $LiMn_2O_4$ (W/O volume ratio = 1/5) and $LiMn_{1.8}Co_{0.2}O_4$ (system I, II, III) are shown in Fig. 7. The first charge and discharge capacities of the undoped $LiMn_2O_4$ were 120.5 and 115.6 mAh/g, respectively [see Fig. 7(a)]. After 30 cycles, the discharge capacity decreased to 102.9 mAh/g, and the capacity retention was only 89%. For the $LiMn_{1.8}Co_{0.2}O_4$ specimen in system I, the first discharge capacity was 105.8 mAh/g and that of the 30th cycle was 103.2 mAh/g [see Fig. 7 (b)], indicating that the capacity retention of system I after cycling was as high as 97.5%. In addition, the discharge capacity of system I was higher than that of the powders having the same composition prepared by sol-gel process.[26] In system II and III, the first discharge capacities of $LiMn_{1.8}Co_{0.2}O_4$ dropped to 80.8 and 70.6 mAh/g, respectively [see Fig. 7(c) and (d)]. As shown in Fig. 3, increasing the W/O volume ratio led to an increase in the percentage of the electrochemically inactive Li_2MnO_3, which in turn decreased the amounts of lithium ions that can participate in the intercalation and de-intercalation processes, so that the capacity was lowered accordingly. In addition, the particle size is also considered to play an important role in influencing the capacity. The large $LiMn_{1.8}Co_{0.2}O_4$ particles obtained at a high W/O volume ratio constituted a greater diffusion barrier for lithium ions diffusing in and out of the spinel compound during the charging and discharging processes, thereby reducing their capacity.

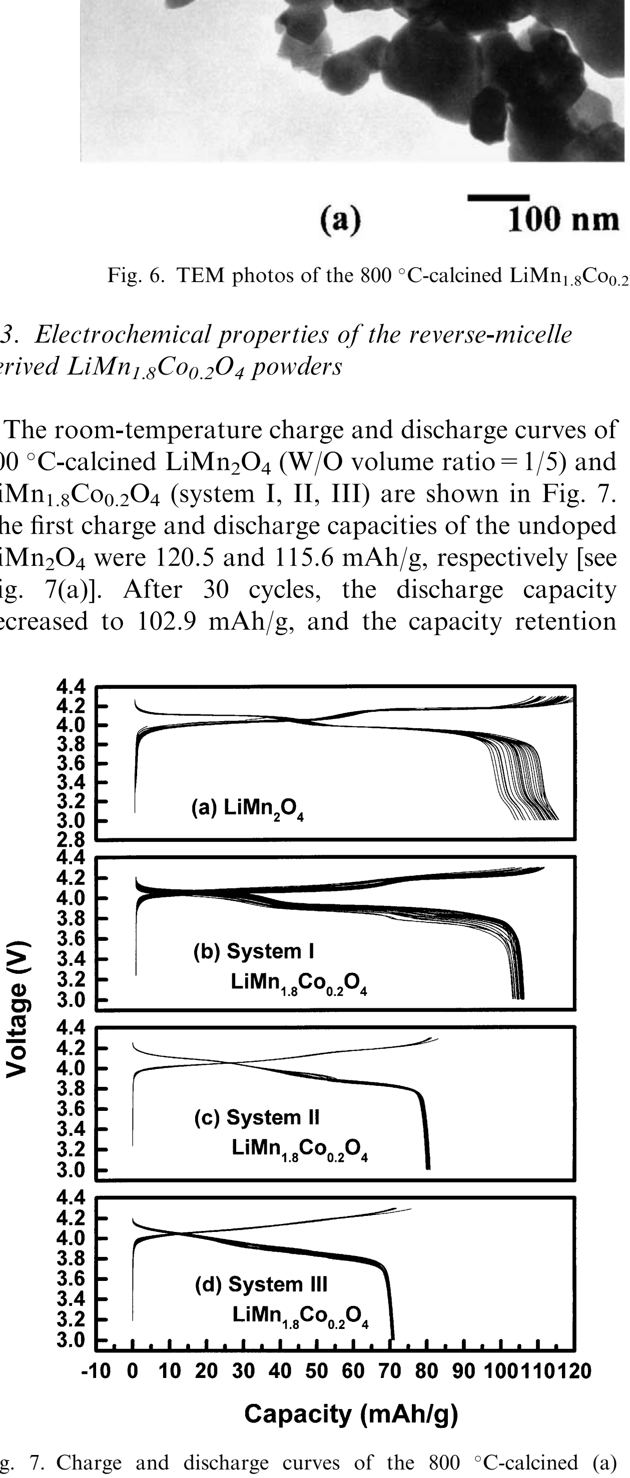

Fig. 7. Charge and discharge curves of the 800 °C-calcined (a) $LiMn_2O_4$ powders and $LiMn_{1.8}Co_{0.2}O_4$ powders prepared at a W/O volume ratio of (b) 1/5, (c)1/1, and (d) 2/1.

Based on the earlier results, it is obvious that the cobalt ion-doped lithium manganate (system I) exhibited excellent cycleability and maintained nearly the initial discharge capacity after 30 cycles. With doping cobalt ions into the spinel structure, the proportion of Mn^{3+} in the spinel compound is lowered, which will reduce the Jahn–Teller effects in the spinel skeleton.[27] Moreover, the bonding energy of Co–O (1067 kJ/mol) in the spinel structure is higher than that of the original Mn–O (946 kJ/mol).[11] Therefore, with doping Co^{3+} into the spinel, the trivalent cations on the octahedral sites of $LiMn_{1.8}Co_{0.2}O_4$ will become more stable in the presence of the Co–O bonding, and the spinel structure will become more rigid during the intercalation and deintercalation process, thereby reducing the capacity fading.

The electrochemical characteristics of the prepared powders at elevated temperature were also investigated. Fig. 8 illustrates the charge and discharge characteristics of the undoped $LiMn_2O_4$ and $LiMn_{1.8}Co_{0.2}O_4$ in system I at 55 °C. Fig. 9 shows the relationship of the discharging capacities of these cathode materials versus the cycle number. The first discharge capacities of $LiMn_2O_4$ and $LiMn_{1.8}Co_{0.2}O_4$ were 99.8 and 93.5 mAh/g, respectively. After 30 cycles, the discharge capacity and the corresponding retention of $LiMn_2O_4$ were 80.8 mAh/g and 80.96%, whereas those of $LiMn_{1.8}Co_{0.2}O_4$ were 90.2 mAh/g and 96.47%, respectively. In comparison with the electrochemical performance at room temperature shown in Fig. 7, the capacity of $LiMn_2O_4$ suffered a serious fading at 55 °C; however, $LiMn_{1.8}Co_{0.2}O_4$ still possessed good capacity retention even at high temperature. The above results revealed that the capacity fading of the spinel compound was apparently improved at ambient and elevated temperatures with the doping of cobalt ions. The reverse-micelle process is demonstrated to be a promising method for preparing other cathode materials of Li-ion secondary batteries.

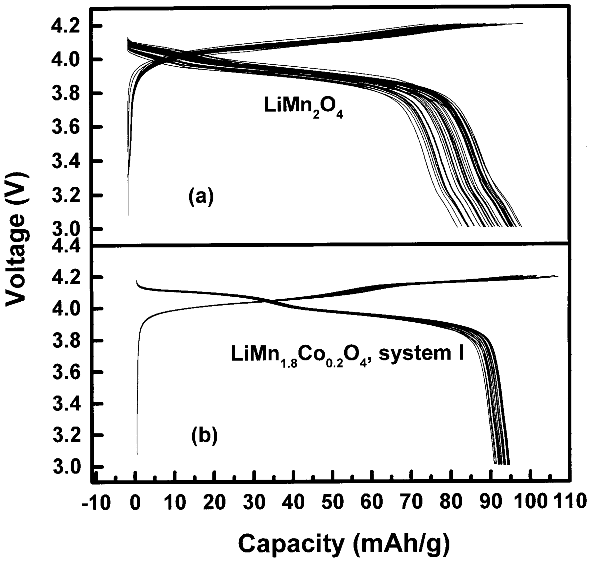

Fig. 8. Charge and discharge curves of the 800 °C-calcined (a) $LiMn_2O_4$ and (b) $LiMn_{1.8}Co_{0.2}O_4$ powders at 55 °C. Both powders were prepared at a W/O volume ratio of 1/5.

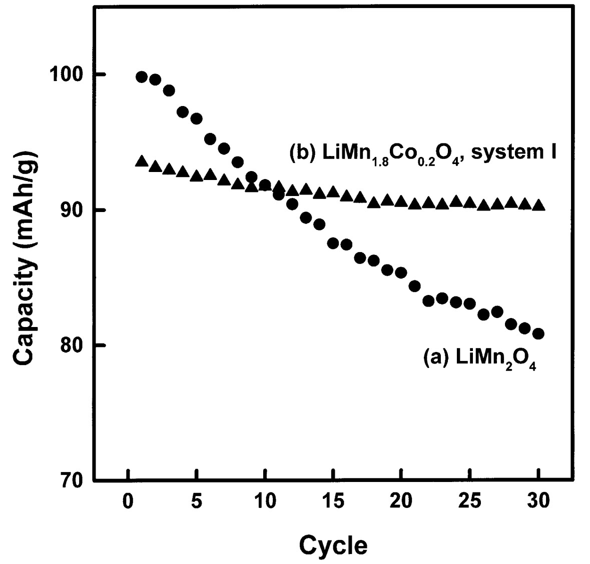

Fig. 9. Cycling stability of 800 °C-calcined (a) $LiMn_2O_4$ and (b) $LiMn_{1.8}Co_{0.2}O_4$ powders at 55 °C, where both powders were prepared at a W/O volume ratio of 1/5.

4. Conclusions

Cobalt ion-doped lithium manganate powders serving as the cathode material in Li-ion batteries have been successfully prepared by a newly developed reverse-micelle process. After calcining the precursors at 500 °C for 2 h, monophasic $LiMn_{1.8}Co_{0.2}O_4$ powders with a Fd3m structure were obtained.

Heating at higher temperatures resulted in an increase in the crystallinity of the powders. The W/O volume ratio was found to be a determinant factor for synthesizing $LiMn_{1.8}Co_{0.2}O_4$. Increasing the W/O volume ratio led to an increase in the particle size of $LiMn_{1.8}Co_{0.2}O_4$ and the formation of an impure Li_2MnO_3 phase. When the W/O volume ratio was 1/5, nanosized, monophasic powders were formed. Doping cobalt ions into the spinel structure slightly decreased the discharge capacity. However, the degree of capacity fading during cycling was successfully reduced at ambient and elevated temperatures.

Acknowledgement

The authors would like to thank Dr. Saha for his assistance in synthesizing the powders utilized in this study.

References

1. Guyomard, D. and Tarascon, J. M., The carbon/$Li_{1+x}Mn_2O_4$ system. *Solid State Ionics*, 1994, **69**, 222–237.
2. Richard, M. N., Fuller, E. W. and Dahn, J. R., The effect of ammonia reduction on the spinel electrode materials, $LiMn_2O_4$ and $Li(Li_{1/3}Mn_{5/3})O_4$. *Solid State Ionics*, 1994, **73**, 81–91.
3. Tarascon, J. M., Mckinnon, W. R., Coowar, F., Bowmer, T. N., Amatucci, G. and Guyomard, D., Synthesis conditions and oxygen stoichiometry effects on Li insertion into the spinel $LiMn_2O_4$. *J. Electrochem. Soc.*, 1994, **141**(6), 1421–1431.
4. Guyomard, D. and Tarascon, J. M., Li metal-free rechargeable $LiMn_2O_4$/carbon cells: Their understanding and optimization. *J. Electrochem. Soc.*, 1992, **139**, 937–947.
5. Thackeray, M. M., Horn, Y. S., Kahaian, A. J., Kepler, K. D., Skinner, E., Vaughey, J. T. and Hackney, S. A., Structural fatigue in spinel electrodes in high voltage (4 V) $Li/Li_xMn_2O_4$ cells. *Electrochem. Solid State Lett.*, 1998, **1**, 7–9.

6. Xia, Y. and Yoshio, M., Optimization of spinel $Li_{1+x}Mn_{2-y}O_4$ as a 4 V Li-cell cathode in terms of a Li-Mn-O phase diagram. *J. Electrochem. Soc.*, 1997, **144**(12), 4186–4194.
7. Jang, D. H. and Oh, S. M., Effects of carbon additives on spinel dissolution and capacity losses in 4V $Li/Li_xMn_2O_4$ rechargeable cells. *Electrochim. Acta*, 1998, **43**, 1023–1029.
8. Pasquier, A. D., Blyr, A., Courjal, P., Larcher, D., Amatucci, G., Gerand, B. and Tarascon, J. M., Mechanism for limited 55 °C storage performance of $Li_{1.05}Mn_{1.9504}$ electrodes. *J. Electrochem. Soc.*, 1999, **146**, 428–436.
9. Arora, P., White, R. E. and Doyle, M., Capacity fade mechanisms and side reactions in lithium-ion batteries. *J. Electrochem. Soc.*, 1998, **145**, 3647–3667.
10. Pistoia, G., Antonini, A., Rosati, R., Bellitto, C. and Ingo, G. M., Doped Li–Mn spinels: physical/chemical characteristics and electrochemical performance in Li-batteries. *Chem. Mater.*, 1997, **7**, 1443–1450.
11. Guohua, L., Ikuta, H., Uchida, T. and Wakihara, M., The spinel phases $LiM_yMn_{2-y}O_4$ (M = Co, Cr, Ni) as the cathode for rechargeable lithium batteries. *J. Electrochem. Soc.*, 1996, **143**, 178–182.
12. Hayashi, N., Ikuta, H. and Wakihara, M., Cathode of $LiMg_yMn_{2-y}O_4$ and $LiM_yMn_{2-y}O_4$-spinel phases for lithium secondary batteries. *J. Electrochem. Soc.*, 1999, **146**, 1351–1354.
13. Arora, P., Popov, B. N. and White, R. E., Electrochemical investigations of cobalt-doped $LiMn_2O_4$ as cathode material for lithium-ion batteries. *J. Electrochem. Soc.*, 1998, **145**, 807–814.
14. Chang, S. H., Ryu, K. S., Kim, K. M., Kim, M. S., Kim, I. K. and Kang, S. G., Electrochemical properties of cobalt-exchanged spinel lithium manganese oxide. *J. Power Sources*, 1999, **84**, 134–173.
15. Amarilla, J. M., Martin, J. L., Vidales, D. and Rojas, R. M., Electrochemical characteristics of cobalt-doped $LiCo_yMn_{2-y}O_4$ ($0 \leq y \leq 0.66$) spinels synthesized at low temperature from $Co_xMn_{3-x}O_4$. *Solid State Ionics*, 2000, **127**, 73–81.
16. Banov, B., Todorov, Y., Trifonova, A., Momchilov, A. and Manev, V., $LiMn_{2-x}Co_xO_4$ cathode with enhanced cycleability. *J. Power Sources*, 1997, **68**, 578–581.
17. Mehrens, W. M., Butz, A., Oesten, R., Arnold, G., Hemmer, R. P. and Hugins, R. A., The influence of doping on the operation of lithium manganese oxide spinel. *J. Power Sources*, 1997, **68**, 582–585.
18. Franger, S., Bach, S., Ramos, P. P. J. and Baffier, N., Chemistry and electrochemistry of low-temperature manganese oxide as lithium intercalation compounds. *J. Electrochem. Soc.*, 2000, **147**(9), 3226–3230.
19. Lu, C. H. and Yeh, P. Y., Ultrafine lithium cobalt oxide powder derived from a water-in-oil emulsion process. *J. Mater. Chem.*, 2000, **10**, 599–601.
20. Takayuki, H., Jun, K. and Isao, K., Preparation of acicular ferrite fine particles using an emulsion liquid membrane system. *Langmuir*, 1999, **15**(19), 6291–6298.
21. Tai, C. Y., Lee, M. H. and Lu, C. H., Synthesis of spherical zirconia by precipitation between two water/oil emulsions. *J. Eur. Ceram. Soc.*, 1999, **19**(15), 2593–2603.
22. Haram, S. K., Mahadeshwar, A. R. and Dixit, S. G., Synthesis and characterization of copper sulfide nanoparticles in Triton-X 100 water-in-oil microemulsions. *J. Phys. Chem.*, 1996, **100**, 5868–5873.
23. Sevinc, I., Sarikaya, Y. and Akinc, M., Adsorption characteristics of alumina powders produced by emulsion evaporation. *Ceram. Int.*, 1991, **17**, 1–4.
24. Cullity, B. D., Elements of X-ray Diffraction, 2nd edn. Addison-Wesley, 1978.
25. Hernan, L., Morales, J., Sanchez, L. and Santos, J., Electrochemical properties of defective $Li_{1-x}Mn_{2-\delta}O_4$ spinels prepared by a sol-gel method used as cathodes in lithium cells. *Solid State Ionics*, 1997, **104**, 205–213.
26. Hernan, L., Morales, J., Sanchez, L. and Santos, J., Use of Li–M–Mn–O [M = Co, Cr, Ti] spinels prepared by a sol-gel method as cathodes in high-voltage lithium batteries. *Solid State Ionics*, 1999, **118**, 179–185.
27. Yamada, A., Tanaka, M., Tanaka, K. and Sekai, K., Jahn-Teller instability in spinel Li-Mn-O. *J. Power Sources*, 1999, **81–82**, 73–78.